Umbelliferone Decorated Water-soluble Zinc(II) Phthalocyanines – *In Vitro* Phototoxic Antimicrobial Anti-cancer Agents

Andrea Sowa,[a] Alexander Höing,[b] Ulrich Dobrindt,[c] Shirley K. Knauer,[b] Anzhela Galstyan,*[d] and Jens Voskuhl*[a]

Abstract: In this contribution we report on the synthesis, characterization and application of water-soluble zinc(II) phthalocyanines, which are decorated with four or eight umbelliferone moieties for photodynamic therapy (PDT). These compounds are linked peripherally to zinc(II) phthalocyanine by a triethylene glycol linker attached to pyridines, leading to cationic pyridinium units, able to increase the water solubility of the system. Beside their photophysical properties they were analyzed concerning their cellular distribution in human hepatocyte carcinoma (HepG2) cells as well as their phototoxicity towards HepG2 cells, Gram-positive (*S. aureus* strain 3150/12 and *B. subtilis* strain DB104) and Gram-negative bacteria (*E. coli* strain UTI89 and *E. coli* strain Nissle 1917). At low light doses and concentrations, they exhibit superb antimicrobial activity against Gram-positive bacteria as well as anti-tumor activity against HepG2. They are even capable to inactivate Gram-negative bacteria, whereas the dark toxicity remains low. These unique water-soluble compounds can be regarded as all-in-one type photosensitizers with broad applications ranges in the future.

Introduction

In these days of increasing pathogen load, which come up with multi drug resistance against antibiotics[1] and unwanted side effects of chemotherapeutics in tumor therapies, alternative treatment methods gain more and more importance.[2] One of these promising approaches is the so-called photodynamic therapy (PDT), which targets cancer cells.[3] A more specialized treatment is the antimicrobial PDT (aPDT), which could be used to inactivate bacteria, algae or yeasts.[4] Although both are already used in the clinics, the demand on efficient, non-toxic, water-soluble and easy to synthesize photosensitizers (PS) remains high.[5]

The idea behind both concepts is based on the "photodynamic effect"[6] and the activation by light of a so-called photosensitizer (PS). From its singlet ground state, the PS is activated to an excited singlet state, which can undergo intersystem crossing to the excited triplet state, followed by a decay to the triplet ground state energy. From this state energy of PS can be transferred to triplet oxygen ($^3O_2$), which leads to the generation of cell toxic singlet oxygen ($^1O_2$). Besides this type II photochemical reaction, a type I reaction can occur as well. In that case the excited triplet state of the PS reacts directly with nearby biomolecules. A hydrogen atom or an electron is subtracted, forming radicals, which can then react with oxygen. Reactive oxygen species (ROS)[7] like superoxide anion radicals ($O_2^{-\bullet}$), hydrogen peroxide (H_2O_2) and hydroxyl radicals ($HO^\bullet$)[8] are formed.[8a,c] They can induce oxidation processes of organic structures and subsequently immediate cell death or apoptosis.[9]

Depending on the application (e.g. injection[7] or superficial application[10]), the requirements concerning the PS have to be chosen individually and should be adapted to the demand of the therapy. For example, if the light to activate the PS needs to pass through the patient's skin the absorption maximum should be within the biological window to allow for a deep penetration depth of the light.[8a] Moreover, among others a good PS should have a high extinction coefficient, low dark toxicity and a high selectivity towards the target (bacteria, tumor cells).[11]

The most common photosensitizers beside others are porphyrins (PORs) and phthalocyanines (PCs).[12a] They absorb

[a] *A. Sowa, Jun.-Prof. J. Voskuhl*
Institute of Chemistry (Organic chemistry)
University of Duisburg-Essen
Universitätsstraße 7, 45117 Essen (Germany)
E-mail: jens.voskuhl@uni-due.de

[b] *A. Höing, Prof. Dr. S. K. Knauer*
Department of Molecular Biology II
Center for Medical Biotechnology (ZMB)
University of Duisburg-Essen
Universitätsstrasse 5, 45117 Essen (Germany)

[c] *Prof. Dr. U. Dobrindt*
Institute of Hygiene
Westfälische Wilhelms-Universität Münster
Mendelstraße 7, 48149 Münster (Germany)

[d] *Dr. A. Galstyan*
Center for Soft Nanoscience
Westfälische Wilhelms-Universität Münster
Busso-Peus-Straße 10, 48149 Münster (Germany)
E-mail: anzhela.galstyan@wwu.de

Supporting information for this article is available on the WWW under https://doi.org/10.1002/chem.202102255

light in the red to near infrared region of the visible spectrum,[4,13] but due to their planar topology they show an intrinsic aggregation tendency in physiological aqueous media.[2,14] Commonly, this favors non-radiative relaxation pathways of the excited states of the PS leading to an inhibition of the singlet oxygen production. Examples for strategies to overcome this drawback are the incorporation of bulky hydrophilic groups on the periphery of the PS or the incorporation of water-insoluble PSs into micelles as well as carrier systems, which allow, due to hydrophobic interactions, the penetration of the lipid bilayer of cell membranes.[14,15] Furthermore, hydrophobic guest molecules in the periphery of a PS can be incorporated inside the hydrophobic cavity of a hydrophilic host molecule. This simultaneously increases the water solubility and the bulky host-guest complex serves as sterically demanding group to prevent the PS from π-π stacking.[12a,16]

In general, the photo-treatment of Gram-negative bacteria is more challenging than of Gram-positive bacteria due to their additional outer phospholipid membrane. In contrast, Gram-positive bacteria feature a thick but porous peptidoglycan layer.[11] Since both have an overall negatively charged cell surface, cationic PSs[4,17] are the compounds of choice for the treatment of bacteria. Due to their opposite surface charges the cationic PSs are more efficiently bound to the bacterial surface and taken up by them. To pass the phospholipid bilayer an amphiphilic character is advantageous. To achieve an effective treatment of the bacteria the PS should bind to or pass through at least one barrier. Moreover, a plunge of the PS inside the oxygen-rich lipid bilayer[11,18] can be desirable, which allows the inactivation of bacteria in very low concentrations and light doses.[11]

Another class of molecules with antibacterial, anti-inflammatory, antiviral,[19] antifungal[20] or anti-cancer properties are coumarins (2*H*-chromen-2-ones).[19,20c] As diverse as their pharmacological activities are their applications in materials science.[19b] Literature examples are known where scientist combine the outstanding optical properties of coumarins and PSs like PORs or PCs.[19b] Concerning the examples including phthalocyanines, most of them are only tested in organic solvents[21] or tend to aggregate in water,[22] are tested only against cancer cells,[21a] bacteria (Gram-negative and Gram-positive)[20a,b,23] and/or fungi[20a,b] or are not even tested *in vitro*.[19a,21f,22,24] In 2014 *Zhou et al.* have investigated a zinc(II) phthalocyanine conjugate with coumarin derivatives for dual photodynamic and chemotherapy. Although the PC was used for the photodynamic effect, a cooperative effect with the coumarin led to a dark toxicity hence a chemotherapeutic effect against human hepatocarcinoma cells (HepG2) (for a literature survey of different PC systems see Table S5, Supporting Information).[21a]

In this publication, we present two of the first water-soluble, positively charged, umbelliferone decorated tetra- and octa-zinc (II) phthalocyanines, which feature an all-in-one behavior. These compounds exhibit superior water solubility, activity against Gram-positive and Gram-negative bacteria as well as HepG2 cells and will be for sure of high interest for future biomedical applications.

Results and Discussion

Synthesis

In this study a four-fold as well as an eight-fold substituted cationic zinc(II) phthalocyanine (Figure 1) were synthesized and investigated according to their photophysical and photodegradation properties. The halogenated 7-hydroxycoumarin (umbelliferone) ligand (**I-EO$_3$-Umb**) was synthesized in a three step reaction route according to known literature procedures[25] (Scheme S1, Supporting Information). We have chosen triethylene glycol as short flexible linker to increase the water solubility of the molecule. Furthermore, they contribute to the hydrophilic-hydrophobic balance of the final phthalocyanines.

The synthesis of the tetra-substituted zinc(II) phthalocyanine (**ZnOPy$_4$-(EO$_3$-Umb)$_4$**) proceeds over a three step synthesis (Scheme S2, Supporting Information), which starts from commercially available 4-nitrophthalonitrile and 3-hydroxypyridine. In a nucleophilic aromatic substitution reaction[26] in the presence of dry finely ground potassium carbonate, 4-(pyridine-3-yloxy)phthalonitrile was formed. The phthalonitrile was isolated by precipitation in 92% yield. The cyclotetramerization with zinc(II) acetate and catalytic amounts of 1,8-diazabicyclo [5.4.0]undec-7-ene (DBU) in 1-pentanol was performed in accordance to a literature known cyclization reaction with zinc(II).[27] The crude intermediate (**ZnOPy$_4$**) was isolated after column chromatography on silica gel as well as size exclusion chromatography on Sephadex LH-20. Due to broadened signals in the NMR (due to strong aggregation) the intermediate was directly quaternized with **I-EO$_3$-Umb**. To ensure a complete conversion to the tetra-substituted phthalocyanine, the reaction mixture was stirred at 70 °C for 14 d. After size exclusion chromatography on Sephadex LH-20, the product **ZnOPy$_4$-(EO$_3$-Umb)$_4$** was obtained in 98% yield. Since regioisomers could not be separated by size exclusion chromatography the product was used as mixture of different regioisomers as obtained by cyclotetramerisation. Well separated signals without further impurities in the ^{1}H NMR spectrum were detected (Figure S9, Supporting Information). The structure of the new zinc(II) phthalocyanine was confirmed by 1D- and 2D NMR, Fourier-transformed infrared (FTIR) (Figure S21, Supporting Information) and high-resolution mass spectrometry (HRMS) (Figure S17–S18 Supporting Information). In the FTIR spectrum the appearance of new absorption bands of the carbonyl function of the umbelliferone lactone ring (–C=O) at 1720 and 1707 cm^{-1} are observed, which is in well accordance with the literature.[21h]

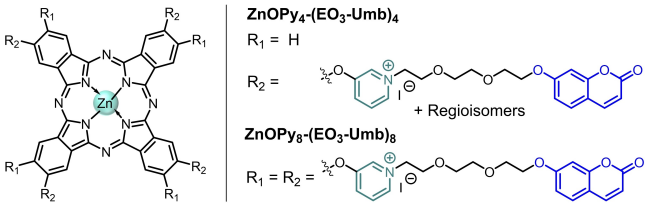

Figure 1. Chemical structure of the zinc(II) phthalocyanines **ZnOPy$_4$-(EO$_3$-Umb)$_4$** and **ZnOPy$_8$-(EO$_3$-Umb)$_8$** used in this study.

Furthermore, during the ionization process in the mass spectrometry counter ions are removed showing masses for the molecular ion minus four iodides (Figure S17–S18, Supporting Information).

The octa-substituted zinc(II) phthalocyanine (**ZnOPy$_8$-(EO$_3$-Umb)$_8$**) was synthesized in a three-step synthesis route (Scheme S3, Supporting Information). Firstly, the commercially available 4,5-dichlorophthalonitrile was converted in a nucleophilic substitution reaction[28] into 4,5-*Bis*(pyridin-3-yloxy) phthalonitrile (**CN$_2$-OPy$_2$**). After flash column chromatography on silica gel the product was obtained in 91% yield, which is higher than stated in the known literature procedure.[27] The cyclotetramerization of the dinitrile with zinc(II) acetate proceeded with a higher yield (57%) than for the previously discussed **ZnOPy$_4$**. This could be due to the purification step, which was changed to washing and centrifugation instead of column chromatography. The last step was the quaternization with **I-EO$_3$-Umb**, which was completed after 14 d at 70 °C. After purification by size exclusion chromatography on Sephadex LH-20 the product **ZnOPy$_8$-(EO$_3$-Umb)$_8$** was obtained in 81 % yield. The resulting product was analyzed by 1D- (Figure 2 and Figure S15–S16, Supporting Information) as well as 2D NMR spectra and mass spectrometry (Figure 2 and Figure S19–S20, Supporting Information).

As already observed for the tetra-substituted compound, the ^{1}H NMR spectrum of **ZnOPy$_8$-(EO$_3$-Umb)$_8$** shows separated signals without impurities, too. Moreover, in the FTIR spectrum the appearance of the coumarin carbonyl band of the lactone ring is observed at 1722 and 1707 cm^{-1}. The mass spectrometric analyses showed molecular ions partially freed from counter ions. Figure 2 shows the spectrum of the most intense peak for [M-5I]$^{5+}$, which agrees very well with the calculated spectrum. Additionally, 1D- and 2D NMR spectra as well as FTIR spectra confirmed the successful synthesis of the compound.

Photophysical characterization

To study the aggregation behavior of the compounds, electronic absorption spectra (UV-vis) were recorded. Both phthalocyanines were investigated in concentrations from 0.25 μM to 10 μM in three different solvents, namely water, phosphate buffered saline (PBS) and *N,N'*-dimethylformamide (DMF). Here solutions in PBS are the most interesting ones, since these conditions are the closest to biological media. The results are listed in Table 1. The corresponding spectra are shown in the Supporting Information (Figure S23, Supporting Information).

Characteristically two strong absorption bands are detected in substituted phthalocyanines, the Q-band at around 600–700 nm[22] and the B- or *Soret*-band at 300–350 nm.[22] H-type aggregation can be detected by a blue shift of the Q-band, accompanied by a decrease of the molar absorption coefficient[21f] as well as a deviation from the Lambert-Beer linear relationship.[29] The tested phthalocyanines **ZnOPy$_4$-(EO$_3$-Umb)$_4$** and **ZnOPy$_8$-(EO$_3$-Umb)$_8$** showed over the whole con-

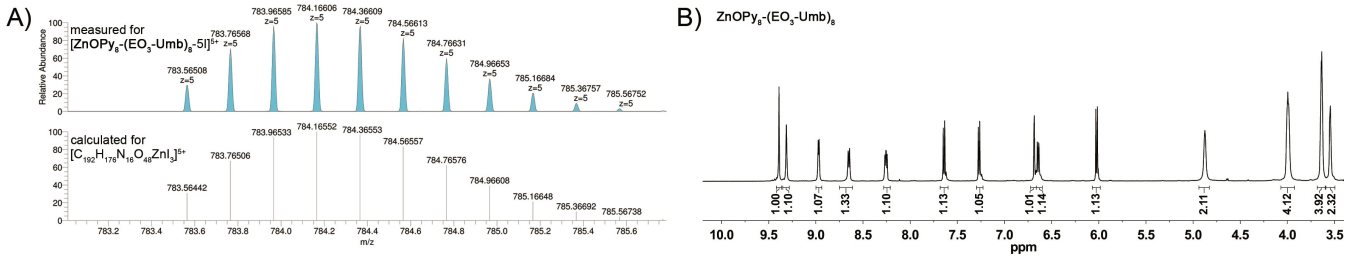

Figure 2. (A) Excerpt of the HR-ESI-MS spectrum with measured and calculated traces of **ZnOPy$_8$-(EO$_3$-Umb)$_8$** and (B) ^{1}H NMR spectrum in DMSO-d_6 of **ZnOPy$_8$-(EO$_3$-Umb)$_8$**.

Table 1. Photophysical parameters of **ZnOPy$_4$-(EO$_3$-Umb)$_4$** and **ZnOPy$_8$-(EO$_3$-Umb)$_8$** in water, PBS and DMF (* Q-band).

Compound Solvent	$\lambda_{Abs.}$/nm ($\log_{10}\varepsilon$)[a]	λ_{Ex}/nm[a]	λ_{Em}/nm[a]	Stokes-shift[a] λ/nm	$\tilde{\nu}$/cm^{-1}	Φ_Δ[b]	Φ_F[c]
ZnOPy$_4$-(EO$_3$-Umb)$_4$							
H_2O	683 (5.15)*, 614 (4.44), 326 (4.88), 289 (4.72)	684	691	8	170	0.52 ± 0.09[d]	0.17 ± 0.05
PBS	683 (4.89)*, 616 (4.32), 326 (4.76), 288 (4.60)	684	691	8	170	0.05 ± 0.02[d]	0.03 ± 0.01
DMF	679 (5.27)*, 671 (5.24)*, 608 (4.54), 327 (4.94)	679	683	4	86	0.57 ± 0.03[e]	0.19 ± 0.04
		671	684	13	283	–	–
ZnOPy$_8$-(EO$_3$-Umb)$_8$							
H_2O	681 (5.29)*, 614 (4.51), 323 (5.08), 289 (4.99)	682	687	6	128	0.64 ± 0.09[d]	0.15 ± 0.08
PBS	682 (5.21)*, 616 (4.20), 323 (5.00), 288 (4.91)	684	689	7	149	0.12 ± 0.04[d]	0.05 ± 0.01
DMF	678 (5.35)*, 611 (4.57), 325 (5.14), 293 (5.01)	677	683	5	108	0.44 ± 0.02[e]	0.17 ± 0.05

[a] Values for solutions with a concentration of $c = 1.0$ μM. [b] ROS quantum yields were measured using the relative method. The values are the mean ± standard deviation of three replicates. [c] Fluorescence quantum yields were measured using an integrating sphere. The results are the mean ± standard deviation in a concentration range of 0.5–10 μM. [d] ADMDMA was used as reactive trap and methylene blue ($\Phi_\Delta = 0.52$)[35] as reference. [e] DPBF was used as reactive trap and unsubstituted zinc(II) phthalocyanine (ZnPC) ($\Phi_\Delta = 0.56$)[36] as reference.

centration range in all solvents sharp Q-bands between 678–683 nm accompanied by a vibrational band[30] at 608–616 nm, which is typical for monomers in solution.[18] Only **ZnOPy$_4$-(EO$_3$-Umb)$_4$** showed in DMF a split of the Q-bands, which is typical for metal free phthalocyanines.[31] But the difference between both maxima (8 nm) is just visible at low scan rates and is much less significant than for metal free phthalocyanines, where the difference between the two bands is in the range of 30–35 nm.[31] Since there is no decrease in the molecular absorption coefficient detectable and the mass spectrum showed the molecular ion with zinc(II) in the center, the Q-band split is supposed to occur due to different regioisomers in the sample. Compared to unsubstituted phthalocyanine (λ_{abs} = 670 nm; log (ε) = 5.37)[32] a bathochromic shift (9 respectively 8 nm) of the Q-band in DMF is observed for the tetra- as well as the octa-substituted phthalocyanine. This phenomenon is known for phthalocyanines with oxygen bridged groups in the periphery.[21f] This bathochromic shift increases if the solvent is changed to water or PBS (Table 1). The B-bands of the phthalocyanines are located in the range of 288–327 nm. Due to an overlap of the B-band of the PC core and the coumarin substituents in that region, bands are broadened.[21a,33]

Furthermore, all absorption maxima and molar absorption coefficients agree very well with the literature.[24,29,32,34] The lowest molar absorption coefficients are found for PBS followed by water and the highest were determined in DMF, which correlates with the solubility of the compounds in these solvents. Moreover, a linear correlation of the Lambert-Beer law is found for both phthalocyanines in water, PBS and DMF, suggesting that they are present in their monomeric form.[29]

Starting from the absorption data, fluorescence spectra were recorded. As shown in Figure 3 the absorption and excitation spectra of both PCs coincide with each other. This is also true for the spectra recorded in PBS and DMF (Figure S24, Supporting Information). The emission spectra are mirror images of the excitation- and absorption spectra. The shape of the recorded spectra is in agreement with previously reported spectra for coumarin substituted zinc(II) phthalocyanines.[21a]

Interestingly, the excitation- and emission spectra start to vary at high concentrations. A splitting of the Q-bands is observed by formation of a blue shifted and a red shifted band. This starts at concentrations greater than 3.0 to 5.0 μM (Figure S25–S26, Supporting Information) indicating that at high concentrations interactions between the molecules and their substituents takes place. All recorded maxima of the excitation- and emission spectra as well as the calculated Stokes-shifts for solutions at 1.0 μM are summarized in Table 1.

As stated in Table 1, the calculated Stokes-shifts between the absorption and the emission wavelength are relatively narrow but comparable to values for zinc(II) phthalocyanine complexes in the literature.[24,32,34]

The determination of the absolute fluorescence quantum yields (Φ_F) (Table 1 and Figure S27, Supporting Information) were performed in an integrating sphere. While the values are comparable for the measurements for **ZnOPy$_4$-(EO$_3$-Umb)$_4$** respectively **ZnOPy$_8$-(EO$_3$-Umb)$_8$** in water (0.17 and 0.15) and DMF (0.19 and 0.17), a decrease of the fluorescence quantum yield is observed in PBS (0.03 and 0.05). Moreover, it was observed that the Φ_F values do not vary with the concentration (0.5–10 μM) if the absorption factor is high enough. If there is nearly no absorption measureable the values differ drastically. This is the reason why for the values in Table 1 the values for 0.25 μM solutions were excluded. The results imply that an aqueous medium does not induce significant aggregation or quenching of the excited-state of the PS. But, it must be taken in mind, that a higher salt concentration like in PBS can cause aggregation or quenching effects. Nevertheless, it is well known that PCs tend to disaggregation upon binding to proteins or when they are taken up by cells.[37] This can lead to reactivation of phototoxic properties.

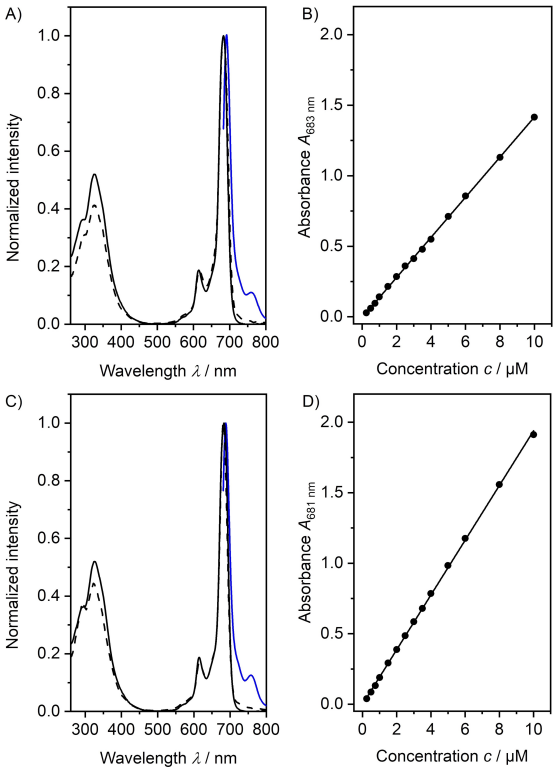

Figure 3. Absorption- (–; black), excitation (- - -) and emission (–; blue) spectra of (A) **ZnOPy$_4$-(EO$_3$-Umb)$_4$** and (C) **ZnOPy$_8$-(EO$_3$-Umb)$_8$** (1.0 μM in H_2O). Lambert-Beer law verified at λ_{max} of (B) **ZnOPy$_4$-(EO$_3$-Umb)$_4$** and (D) **ZnOPy$_8$-(EO$_3$-Umb)$_8$**.

It is known that low fluorescence quantum yields can be an indicator for high singlet oxygen quantum yields (Φ_Δ).[11] Singlet oxygen ($^1O_2$) is considered as the main species involved in PDT, as the most potent PSs have high Φ_Δ values.[18] Even in the aPDT the predominant process is based on type II processes.[17] However, type I reactions are favored if Gram-negative bacteria should be targeted cause they are more susceptible to $^\bullet$OH than $^1O_2$.[17] The Φ_Δ were measured utilizing the relative method.[36] As reactive traps for $^1O_2$ we have used 9,10-anthacenyl-bis(methylene)dimalonic acid (ADMDMA)[18] in aqueous media (water and PBS) and 1,3-diphenylisobenzofuran (DPBF)[18] in DMF. Depending on the solvents, soluble reference substances with literature known Φ_Δ were used. In organic

solvents unsubstituted zinc(II) phthalocyanine (ZnPC) ($\Phi_\Delta = 0.56$)[36] and in aqueous solutions methylene blue (MB) ($\Phi_\Delta = 0.52$)[35] served as references. Control measurements were performed under the same conditions without addition of the photosensitizer.

ADMDMA reacts with $^1O_2$ to its non-emissive endoperoxide.[38] Due to the fact that ADMDMA has more than one emission maximum the decay of the emission intensity integral ($\lambda_{EM} = 380–550$ nm, $\lambda_{EX} = 370$ nm) was determined as function of the irradiation time *t* (Figures S29 and S31, Supporting Information). For the measurements in DMF, DPBF served as trapping-agent. It reacts with $^1O_2$ as well as superoxide anion radicals ($O_2^{\bullet-}$) to form *o*-dibenzoylbenzene (DBB), which destroys the π-system of the isobenzofuran.[39] The formed product is no longer able to absorb or emit visible light.[39] The decay of the absorption maximum at 414 nm can be followed as a function of the irradiation time *t* (Figure S32, Supporting Information).

Highest singlet oxygen quantum yields for **$ZnOPy_4$-(EO_3-Umb)$_4$** were calculated in DMF ($\Phi_\Delta = 0.57$), which is comparable to the unsubstituted reference (ZnPC). The octa-substituted phthalocyanine (**$ZnOPy_8$-(EO_3-Umb)$_8$**) exhibits with 0.44 a 13% lower singlet oxygen quantum yield (Table 1). However, **$ZnOPy_8$-(EO_3-Umb)$_8$** showed the highest value in water ($\Phi_\Delta = 0.64$), which is remarkably higher than the singlet oxygen quantum yield of the reference methylene blue with 0.52.[35] Depending on the aqueous medium the results are better for both species in water than in PBS. For **$ZnOPy_4$-(EO_3-Umb)$_4$** the value decreases from 0.52 in water to 0.05 in PBS, while for **$ZnOPy_8$-(EO_3-Umb)$_8$** it decreases from 0.64 to 0.12 respectively. The extent of exciton coupling increases for closely stacked molecules, which influences the rate of non-radiative relaxation leading to a reduction in ROS formation. In water symmetrically spaced positive charges in the close proximity to the phthalocyanine macrocycle contribute to the monomerization of the dyes. Strong dependence of ROS generation from the media indicates the formation of aggregates caused by the high ionic strength of PBS. This goes along with a minor reduction of the molar absorption coefficient ε, indicating the potential presence of some aggregates in the solution. This phenomenon was already described in the literature, whereby the aggregation tendency was much larger in these cases and was already visible in the UV-vis spectra.[24,34b, 40]

Since cells and bacteria are cultivated in PBS the values in PBS will have more relevance for in vitro tests. A slight aggregation tendency in this medium is not a limitation for the application as PS for PDT, since it is known that PCs tend to disaggregation while taken up by cells or upon binding to proteins.[41]

From the literature it is known that the Φ_Δ decrease in water[16b,34a] or PBS[34b] compared to DMSO[34] or DMF.[21a] Compared to the literature the results in DMF as well as PBS are in an equal range than the results for coumarin tetra-substituted zinc(II) phthalocyanines.[21a,24] Values in water were often measured together with Triton X-100 to induce monomerization to increase the Φ_Δ to measurable values and are therefore not comparable.[34a]

Cell culture experiments

The cytotoxicity of the molecules was investigated in human hepatocarcinoma cells (HepG2). To examine if the phthalocyanines were internalized into the cells, we performed live cell imaging using CLSM (confocal laser scanning microscopy). To differentiate between cellular compartments the nuclei were stained with Hoechst 33342 and the cytoplasm with CellBrite® Green. The cells were then incubated for 30 min at 37 °C in phthalocyanine containing media. The CLSM images (Figure 4 and Figure S33, Supporting Information) showed that both phthalocyanines were internalized. Remarkably, both compounds were not only present in the cytoplasm, but even seemed to accumulate at distinct structures inside the nucleus in a pattern that resembled intranuclear domains like the nucleoli. To further evaluate the internalization of the compounds, we generated image stacks. Of note, this was a demanding task using live cell microscopy due to the photodynamic nature of the compound. However, we succeeded to generate tomographic videos and 3D images of the cells (Figures S34–S35 and videos S1–S2, Supporting Information). Slices through these models show, that the compounds are completely surrounded by the cytoplasmic stain and the presumably intranuclear accumulations are indeed located in the nucleus.

Figure 5 shows the dose and concentration dependent survival values for both phthalocyanines at concentrations of 1 μM and 10 μM upon irradiation with >600 nm light. The graphs show that both phthalocyanines exhibit already at low concentrations (1 μM) and light doses (1.1 J/cm^2) a remarkably reduced cell viability. This is an advantage for the patients in later use in the PDT since less drugs and light can be used. Therefore, potential side effects and burns associated with pain are reduced. After irradiation for 15 min at 1.2 mW/cm^2 (1.1 J/cm^2) nearly 80% of the cells died in the presence of **$ZnOPy_4$-(EO_3-Umb)$_4$**, whereas around 60% died when **$ZnOPy_8$-(EO_3-Umb)$_8$** was added.

This indicates that the phototoxicity of the tetra-substituted phthalocyanine is higher in the initial phase. However, regarding longer irradiation times, for example 60 min, the octa-substituted phthalocyanine seems to be more stable and can sufficiently produce reactive oxygen species to kill cells. Additionally, a dark control experiment without irradiation and an irradiation control experiment without photosensitizer have been performed (Figure S36, Supporting Information). During both irradiation control experiments, cell viability was unaffected even after 60 min of irradiation.

At low concentrations of 1 μM no dark toxicity could be monitored. In contrast, at high concentrations such as 10 μM **$ZnOPy_4$-(EO_3-Umb)$_4$** exhibited a minor toxicity (cell viability of around 75%) after 60 min while nearly no dark toxicity was observed for **$ZnOPy_8$-(EO_3-Umb)$_8$** (cell viability of 85%). Of note, while we reduced unwanted light exposure to the possible minimum it was not possible to shield these highly reactive compounds completely during the cell culture application. We therefore performed additional dark experiments for 72 h to investigate if the observed dark toxicity is related to the dark

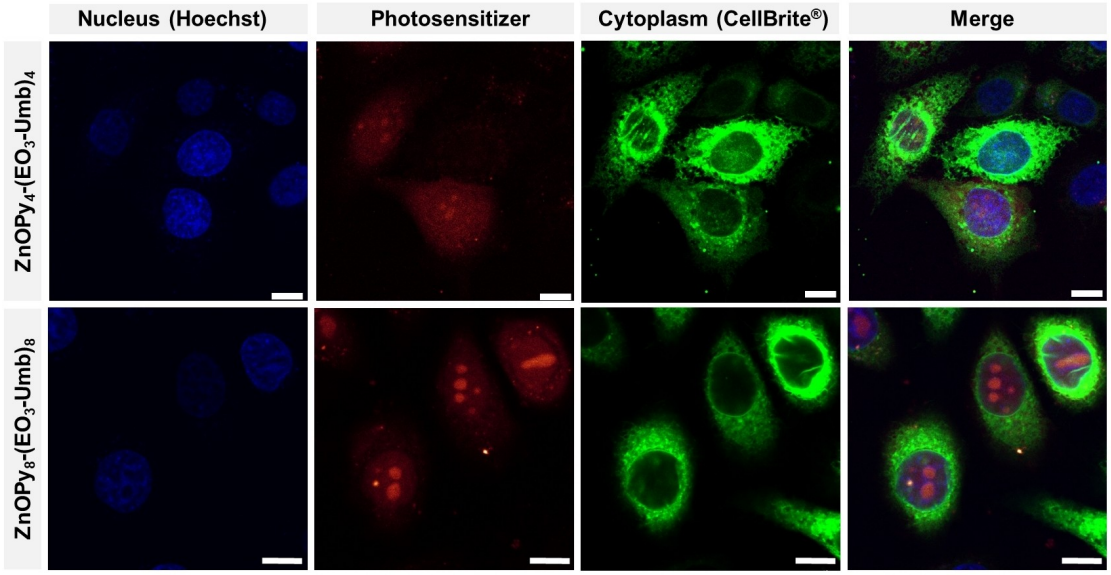

Figure 4. Live cell microscopy images of HepG2 cells treated with **ZnOPy$_4$-(EO$_3$-Umb)$_4$** or **ZnOPy$_8$-(EO$_3$-Umb)$_8$** (red). The nuclei were stained with Hoechst 33342 (blue) and the cytoplasm with CellBrite® Green (green). Scale bars represent 10 μm. See Figure S33 (Supporting Information) for additional images and controls.

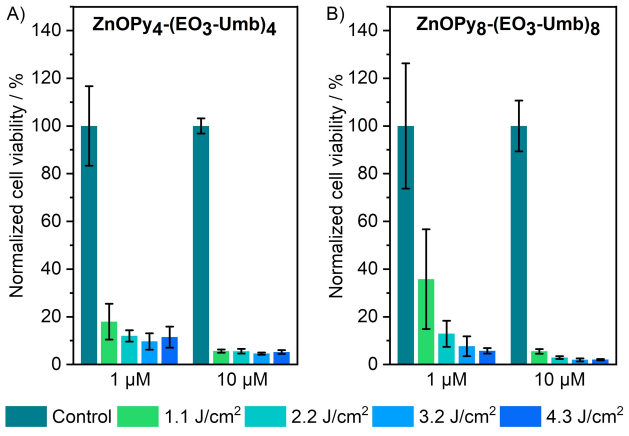

Figure 5. Viability of HepG2 cells after photodynamic treatment with (A) **ZnOPy$_4$-(EO$_3$-Umb)$_4$** or (B) **ZnOPy$_8$-(EO$_3$-Umb)$_8$**. The cells were treated with the respective compound concentrations and then exposed to 1.2 mW/cm^2 light (>600 nm) for 0 min (Control), 15 min (1.1 J/cm^2), 30 min (2.2 /cm^2), 45 min (3.2 J/cm^2) or 60 min (4.3 J/cm^2). Error bars are the mean ± standard deviation from three replicates.

exposure time (Figure S36, Supporting Information). Even after 72 h incubation in compound-supplied medium, the cell viability did not decrease further, indicating the minor dark toxicity observed is unrelated to the dark exposure, but presumably a phototoxic artefact introduced during initial handling.

In vitro antimicrobial experiments

Since it is known that Gram-negative and Gram-positive bacteria have a different composition of outer membranes[11] both type of bacteria were tested. As representative Gram-positive bacteria *B. subtilis* strain DB104 and *S. aureus* strain 3150/12 were used, as well as the Gram-negative *E. coli* strains Nissle 1917 and UTI89. Among these, *S. aureus* strain 3150/12 and *E. coli* strain UTI89 are clinical isolates. To evaluate binding efficacy of **ZnOPy$_4$-(EO$_3$-Umb)$_4$** and **ZnOPy$_8$-(EO$_3$-Umb)$_8$** to microorganisms, fluorescence images were recorded. Therefore, bacterial suspensions labelled with Hoechst 33342 were further incubated with the corresponding photosensitizer for 15 min at 37 °C in the dark. Hoechst 33342 visualizes the DNA inside the bacterial cell membrane while the photosensitizer can be detected by its characteristic red emission. As shown in Figure 6 (Figure S38, Supporting Information), Gram-positive bacteria were uniformly labeled with **ZnOPy$_4$-(EO$_3$-Umb)$_4$** or **ZnOPy$_8$-(EO$_3$-Umb)$_8$**. In the merged images the blue emissive bacteria DNA (Hoechst) and the red emissive photosensitizer nicely overlap.

Although the majority of Gram-negative bacteria were labeled as well, some unstained bacteria were also detected. To evaluate antimicrobial efficiency, bacterial strains were incubated in the dark with the corresponding photosensitizer at 1 μM or 10 μM as final concentration for 15 min at 37 °C and irradiated for 15 or 30 min (660 ± 24 nm). Subsequently serial dilutions were plated on lysogeny broth (LB) agar plates and the number of colony-forming units (CFU) was counted after incubation at 37 °C for 24 h. Within two groups of Gram-positive or Gram-negative bacteria the results for both phthalocyanines are comparable. In Figure 7 the graphs for *B. subtilis* strain DB104 and *E. coli* strain Nissle 1917 are shown (graphs for *E. coli* strain UTI89 and *S. aureus* strain 3150/12 can be found in Figure S37, Supporting Information).

As illustrated in Figure 7, **ZnOPy$_4$-(EO$_3$-Umb)$_4$** and **ZnOPy$_8$-(EO$_3$-Umb)$_8$** are significantly more active against Gram-positive

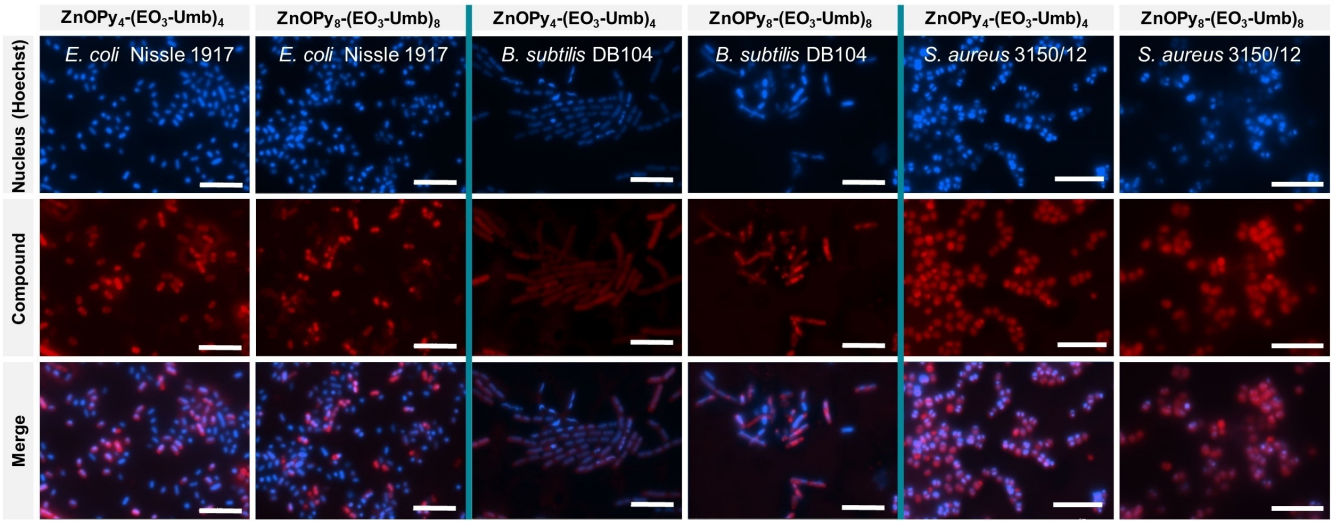

Figure 6. Co-localization of **$ZnOPy_4$-$(EO_3$-Umb$)_4$** and **$ZnOPy_8$-$(EO_3$-Umb$)_8$** (red) with the DNA (blue) in *B. subtilis* strain DB104, *E. coli* strain Nissle 1917 and *S. aureus* strain 3150/12. The scale bars represent a length of 5 μm.

than against Gram-negative bacteria. Even at low concentrations of 1 μM and light doses of 4.5 J/cm^2 $>5\log_{10}$, reduction of viability was observed, while at 10 μM or higher light doses of 9 J/cm^2 no colony forming units can be counted anymore. Interestingly, *B. subtilis* strain DB104 was more suszeptible than *S. aureus* strain 3150/12. Contrary to the previously described HepG2 cells **$ZnOPy_8$-$(EO_3$-Umb$)_8$** is more active than **$ZnOPy_4$-$(EO_3$-Umb$)_4$**. Due to the fact that the surface of bacteria is mostly negatively charged[17] it was expected that **$ZnOPy_8$-$(EO_3$-Umb$)_8$** with eight positive charges will bind better to the surface when compared to four positive charges in **$ZnOPy_4$-$(EO_3$-Umb$)_4$** leading to improved killing of both Gram-positive and negative bacteria.

For Gram-negative bacteria, a significant reduction of colony forming units was just observed at higher concentrations (10 μM). No obvious differences were observed between pathogenic and non-pathogenic *E. coli* strains. Whereby, for both phthalocyanines a light dose dependency was detected. The higher the applied light dose, the higher is the reduction of bacterial colony counts.

For two selected bacterial strains we performed a live/dead assay to visualize the photoinactivation of Gram-positive (*B. subtilis* strain DB104) and Gram-negative bacteria (*E. coli* strain Nissle 1917) (Figure S39, Supporting Information). For *B. subtilis* strain DB104 we discovered a clustering into microcolonies upon incubation and irradiation going along with a full inactivation of the bacteria as detectable by the red emission. In addition, *E. coli* strain Nissle 1917 showed also remarkable inactivation in the presence of the photosensitizers, which was more pronounced for **$ZnOPy_8$-$(EO_3$-Umb$)_8$**, as observable by a higher amount of dead (red) bacteria.

Conclusion

To conclude, two water-soluble tetra- and octa-coumarin substituted zinc(II) phthalocyanines were successfully synthesized and characterized. Their antimicrobial as well as anticancer photodynamic efficiency against human hepatocyte carcinoma (HepG2) cells, Gram-positive and Gram-negative bacteria were investigated. All tested zinc(II) phthalocyanines showed a sharp Q-band and a linear behavior concerning the Lambert-Beer law indicating monomeric species in DMF but also in water and physiological media as PBS. Where others need additional solubilization agents like Triton X-100 our compounds are intrinsically water-soluble. We assume that the coumarin moieties not only contribute to the hydrophilic-lipophilic balance of the molecules promoting their uptake by the cells, but also favor the accumulation of PS in the cell nuclei, as can be seen in the confocal microscopy images. Studies to investigate the origin of this remarkable propensity are currently being carried out in our laboratory. Furthermore, the photophysical parameters as well as the anti-cancer and antimicrobial tests have shown that both species are extremely active upon irradiation. For HepG2 and Gram-positive bacteria low concentrations and minimal light doses are already sufficient to kill most of the cells or bacteria. This may reduce unwanted side effects, the exposure time and the amount of drug which needs to be administered to the patient. Additionally, nearly no dark toxicity was detected in the experiments. Moreover, it is possible to treat Gram-negative bacteria as well, which is more complicated than for Gram-positive bacteria. Even though, higher light doses and concentrations are needed. This suggests potential candidates, which can be used not only in the PDT but also in the aPDT. This allows the drug to be used regardless of whether one aims at targeting cancer cells, Gram-positive or Gram-negative bacteria. This opens up a wide range of possible applications.

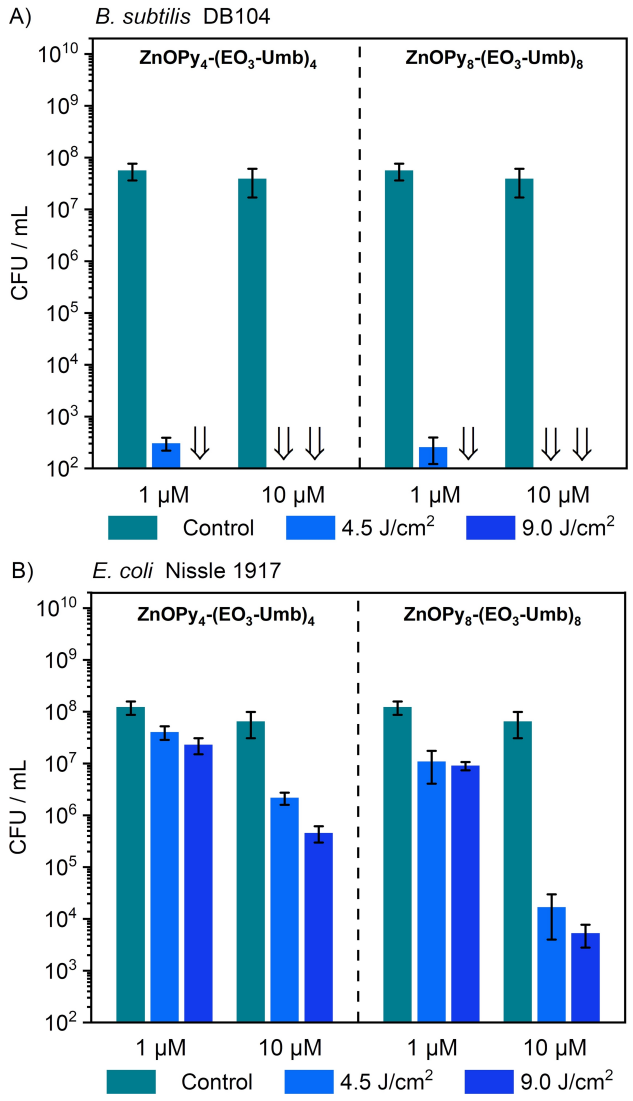

Figure 7. Photoinactivation of (A) Gram-positive *B subtilis* strain DB104 and (B) Gram-negative *E. coli* strain Nissle 1917 with **$ZnOPy_4$-$(EO_3$-Umb$)_4$** and **$ZnOPy_8$-$(EO_3$-Umb$)_8$**. The bacteria were exposed to 5 mW/cm^2 light (> 600 nm) for 15 min (4.5 J/cm^2) or 30 min (9.0 J/cm^2). Control samples did not contain PC and were irradiated for 30 min (9.0 J/cm^2). Error bars are the mean ± standard deviation from three replicates.

Acknowledgements

Jens Voskuhl and Andrea Sowa acknowledge Evonik Industries AG (Funding to AS) as well as the German-Israeli foundation (Grant No. G-2420-302.5/2016 to JV) for financial support. Anzhela Galstyan thanks the Deutsche Forschungsgemeinschaft (Grant No. GA 2362/2-1), Fonds der Chemischen Industrie and WWU Münster for financial support. We acknowledge the use of the imaging equipment and the support of the "Imaging Center Campus Essen" (ICCE). Instrument Leica TCS SP8X FALCON was obtained through DFG funding (Major Research Instrumentation Program as per Art. 91b GG, INST 20876/294-1 FUGG). Open Access funding enabled and organized by Projekt DEAL.

Conflict of Interest

The authors declare no conflict of interest.

Keywords: antimicrobial · antitumor agents · coumarin · photodynamic therapy · phthalocyanines

[1] A. Galstyan, R. Schiller, U. Dobrindt, *Angew. Chem. Int. Ed.* **2017**, *56*, 10362–10366; *Angew. Chem.* **2017**, *129*, 10498–10502.
[2] C. A. Strassert, M. Otter, R. Q. Albuquerque, A. Hone, Y. Vida, B. Maier, L. d. Cola, *Angew. Chem. Int. Ed.* **2009**, *48*, 7928–7931; *Angew. Chem.* **2009**, *121*, 8070–8073.
[3] R. F. Donnelly, P. A. McCarron, M. M. Tunney, *Microbiol. Res.* **2008**, *163*, 1–12.
[4] J. Ghorbani, D. Rahban, S. Aghamiri, A. Teymouri, A. Bahador, *Laser Therapy* **2018**, *27*, 293–302.
[5] a) S. B. Brown, E. A. Brown, I. Walker, *Lancet Oncol.* **2004**, *5*, 497–508; b) X. Hu, Y.-Y. Huang, Y. Wang, X. Wang, M. R. Hamblin, *Front. Microbiol.* **2018**, *9*, 1299.
[6] S. Kwiatkowski, B. Knap, D. Przystupski, J. Saczko, E. Kędzierska, K. Knap-Czop, J. Kotlińska, O. Michel, K. Kotowski, J. Kulbacka, *Biomed. Pharmacother.* **2018**, *106*, 1098–1107.
[7] Y.-Y. Wang, Y.-C. Liu, H. Sun, D.-S. Guo, *Coord. Chem. Rev.* **2019**, *395*, 46–62.
[8] a) P. Agostinis, K. Berg, K. A. Cengel, T. H. Foster, A. W. Girotti, S. O. Gollnick, S. M. Hahn, M. R. Hamblin, A. Juzeniene, D. Kessel, M. Korbelik, J. Moan, P. Mroz, D. Nowis, J. Piette, B. C. Wilson, J. Golab, *CA: A Cancer Journal for Clinicians* **2011**, *61*, 250–281; b) M. M. Kim, A. A. Ghogare, A. Greer, T. C. Zhu, *Phys. Med. Biol.* **2017**, *62*, R1–R48; c) J. Zhang, C. Jiang, J. P. Figueiró Longo, R. B. Azevedo, H. Zhang, L. A. Muehlmann, *Acta Pharmaceut. Sin. B* **2018**, *8*, 137–146.
[9] J. Dubbert, A. Höing, N. Riek, S. K. Knauer, J. Voskuhl, *Chem. Commun.* **2020**, *56*, 7653–7656.
[10] L. P. Rosa, C. da Silva, *J. Med. Microb. Diagn.* **2014**, *03*, 158.
[11] A. Galstyan, U. Dobrindt, *J. Mater. Chem. B* **2018**, *6*, 4630–4637.
[12] a) A. Sowa, J. Voskuhl, *Int. J. Pharm.* **2020**, *586*, 119595; b) A. Galstyan, *Chem. Eur. J.* **2020**, *27*, 1903–1920.
[13] R. Bonnett, *Chem. Soc. Rev.* **1995**, *24*, 19–33.
[14] X.-y. Li, X. He, A. C. H. Ng, C. Wu, D. K. P. Ng, *Macromolecules* **2000**, *33*, 2119–2123.
[15] S. S. Lucky, K. C. Soo, Y. Zhang, *Chem. Rev.* **2015**, *115*, 1990–2042.
[16] a) L. Chen, H. Bai, J.-F. Xu, S. Wang, X. Zhang, *ACS Appl. Mater. Interfaces* **2017**, *9*, 13950–13957; b) J. Voskuhl, U. Kauscher, M. Gruener, H. Frisch, B. Wibbeling, C. A. Strassert, B. J. Ravoo, *Soft Matter* **2013**, *9*, 2453.
[17] Y. Liu, R. Qin, S. A. J. Zaat, E. Breukink, M. Heger, *J. Clin. Transl. Res.* **2015**, *1*, 140–167.
[18] A. Galstyan, J. Putze, U. Dobrindt, *Chem. Eur. J.* **2018**, *24*, 1178–1186.
[19] a) H. Çakıcı, A. A. Esenpınar, M. Bulut, *Polyhedron* **2008**, *27*, 3625–3630; b) A. F. R. Cerqueira, V. A. S. Almodôvar, M. G. P. M. S. Neves, A. C. Tomé, *Molecules* **2017**, *22*, 994.
[20] a) R. Medyouni, A. C. Mtibaa, L. Mellouli, A. Romerosa, N. Hamdi, *J. Inclusion Phenom. Macrocyclic Chem.* **2016**, *86*, 201–210; b) N. Hamdi, R. Medyouni, A. Sulaiman Al-Ayed, L. Mansour, A. Romerosa, *J. Heterocycl. Chem.* **2017**, *54*, 2342–2351; c) K. N. Venugopala, V. Rashmi, B. Odhav, P. W. Doetsch, *BioMed Res. Int.* **2013**, *2013*, 963248.
[21] a) X.-Q. Zhou, L.-B. Meng, Q. Huang, J. Li, K. Zheng, F.-L. Zhang, J.-Y. Liu, J.-P. Xue, *ChemMedChem* **2015**, *10*, 304–311; b) A. A. Esenpınar, A. R. Özkaya, M. Bulut, *J. Organomet. Chem.* **2011**, *696*, 3873–3881; c) A. A. Esenpınar, M. Durmuş, M. Bulut, *Polyhedron* **2011**, *30*, 2067–2074; d) A. A. Esenpınar, M. Durmuş, M. Bulut, *Spectrochim. Acta Part A* **2011**, *81*, 690–697; e) M. Çamur, M. Durmuş, A. Rıza Özkaya, M. Bulut, *Inorg. Chim. Acta* **2012**, *383*, 287–299; f) A. A. Esenpınar, E. Durmaz, F. Karaca, M. Bulut, *Polyhedron* **2012**, *38*, 267–274; g) E. N. Kaya, M. Durmuş, M. Bulut, *J. Porphyrins Phthalocyanines* **2015**, *19*, 1114–1122; h) S. Altun, A. R. Özkaya, M. Bulut, *Polyhedron* **2012**, *48*, 31–42; i) O. Soyer Can, E. N. Kaya, M. Durmuş, M. Bulut, *J. Photochem. Photobiol. A* **2016**, *317*, 56–67.
[22] C. Y. Boyar, M. Çamur, *Inorg. Chim. Acta* **2019**, *494*, 30–41.
[23] N. Hamdi, A. Ben Hsouna, C. Bruneau, R. Medyouni, A. Sulaiman Al-Ayed, H. Ali Soleiman, F. Zaghrouba, *Heterocycles* **2013**, *87*, 2283.
[24] M. Çamur, M. Durmuş, M. Bulut, *Polyhedron* **2012**, *41*, 92–103.

[25] a) J. Motoyanagi, T. Fukushima, A. Kosaka, N. Ishii, T. Aida, *J. Polym. Sci. Part A* **2006**, *44*, 5120–5127; b) J. Motoyanagi, T. Fukushima, N. Ishii, T. Aida, *J. Am. Chem. Soc.* **2006**, *128*, 4220–4221.
[26] M. Spesia, E. Durantini, *Dyes Pigment.* **2008**, *77*, 229–237.
[27] H. Li, T. J. Jensen, F. R. Fronczek, M. G. H. Vicente, *J. Med. Chem.* **2008**, *51*, 502–511.
[28] D. Wöhrle, M. Eskes, K. Shigehara, A. Yamada, *Synthesis* **1993**, *2*, 194–196.
[29] C. A. Strassert, G. M. Bilmes, J. Awruch, L. E. Dicelio, *Photochem. Photobiol. Sci.* **2008**, *7*, 738–747.
[30] A. Galstyan, U. Kauscher, D. Block, B. J. Ravoo, C. A. Strassert, *ACS Appl. Mater. Interfaces* **2016**, *8*, 12631–12637.
[31] a) J. Tant, Y. H. Geerts, M. Lehmann, V. d. Cupere, G. Zucchi, B. W. Laursen, T. Bjørnholm, V. Lemaur, V. Marcq, A. Burquel, E. Hennebicq, F. Gardebien, P. Viville, D. Beljonne, R. Lazzaroni, J. Cornil, *J. Phys. Chem. B* **2005**, *109*, 20315–20323; b) T. Wang, X.-F. Zhang, X. Lu, *J. Mol. Struct.* **2015**, *1084*, 319–325; c) M. Özdemir, F. Aytan Kilicarslan, A. Erdogmus, I. Erden, *J. Chem. Res.* **2016**, *40*, 250–254.
[32] M. Pişkin, M. Durmuş, M. Bulut, *J. Photochem. Photobiol. A* **2011**, *223*, 37–49.
[33] a) X. Zhang, X. Pei, C. Liao, L. Zou, *Res. Chem. Intermed.* **2017**, *43*, 2737–2752; b) A. Alemdar, A. R. Özkaya, M. Bulut, *Synth. Met.* **2010**, *160*, 1556–1565.
[34] a) S. Çolak, M. Durmuş, S. Z. Yıldız, *Polyhedron* **2016**, *113*, 115–122; b) D. Çakır, V. Çakır, Z. Bıyıklıoğlu, M. Durmuş, H. Kantekin, *J. Organomet. Chem.* **2013**, *745–746*, 423–431.
[35] Y. Usui, *Chem. Lett.* **1973**, *2*, 743–744.
[36] W. Spiller, H. Kliesch, D. Wöhrle, S. Hackbarth, B. Röder, G. Schnurpfeil, *J. Porphyrins Phthalocyanines* **1998**, *02*, 145–158.
[37] A. Galstyan, D. Block, S. Niemann, M. C. Grüner, S. Abbruzzetti, M. Oneto, C. G. Daniliuc, S. Hermann, C. Viappiani, M. Schäfers, B. Löffler, C. A. Strassert, A. Faust, *Chem. Eur. J.* **2016**, *22*, 5243–5252.
[38] T. Entradas, S. Waldron, M. Volk, *J. Photochem. Photobiol. B* **2020**, *204*, 111787.
[39] X.-F. Zhang, X. Li, *J. Lumin.* **2011**, *131*, 2263–2266.
[40] L. Alonso, R. N. Sampaio, T. F. M. Souza, R. C. Silva, N. M. B. Neto, A. O. Ribeiro, A. Alonso, P. J. Gonçalves, *J. Photochem. Photobiol. B* **2016**, *161*, 100–107.
[41] A. Galstyan, K. Riehemann, M. Schäfers, A. Faust, *J. Mater. Chem. B* **2016**, *4*, 5683–5691.

Manuscript received: June 23, 2021
Accepted manuscript online: July 29, 2021
Version of record online: September 15, 2021

